Peptide Helicity and Membrane Surface Charge Modulate the Balance of Electrostatic and Hydrophobic Interactions with Lipid Bilayers and Biological Membranes

Margitta Dathe,*,‡ Michael Schümann,‡ Torsten Wieprecht,‡ Anett Winkler,‡ Michael Beyermann,‡ Eberhard Krause,‡ Katsumi Matsuzaki,§ Osamu Murase,§ and Michael Bienert‡

Institute of Molecular Pharmacology, Alfred-Kowalke-Strasse 4, D-10315 Berlin, Germany, and Faculty of Pharmaceutical Sciences, Kyoto University, Sakyo-ku, Kyoto 606-01, Japan

Received April 8, 1996; Revised Manuscript Received July 9, 1996⊗

ABSTRACT: An amphipathic model peptide, KLALKLALKALKAAKLA-NH_2, and its complete double D-amino acid replacement set was used to analyze the process of peptide binding at lipid vesicles of different surface charge and to determine the structure of the lipid-bound peptides using CD spectroscopy. The relationship between peptide helicity, model membrane permeability, and biological activity has been studied by dye release from liposomes and investigation of antibacterial and hemolytic activity. The accumulation of cationic KLAL peptides at and the membrane-disturbing effect on bilayers of high negative surface charge were found to be dominated by charge interactions. Independent of any structural propensity, the cationic peptide side chains bind to the anionic phosphatidylglycerol moieties. The charge interactions hold the peptides at the bilayer surface, where they may disturb preferentially lipid headgroup organization by formation of peptide−lipid clusters. In contrast, KLAL peptide interaction with bilayers of low negative surface charge is highly dependent on peptide helicity. With decreasing amounts of anionic phosphatidylglycerol in the bilayer the membrane-disturbing effect of KLAL and other helical analogs substantially increases despite drastically reduced binding affinity. Less helical peptides exhibit reduced bilayer-disturbing activity, showing that the hydrophobic helix domain is decisive for binding at and inducing permeability in membranes of low negative surface charge. It is suggested that hydrophobic interactions drive the penetration of the amphipathic peptide structure into the inner membrane region, thus disturbing the arrangement of the lipid acyl chains and causing local disruption. On the basis of the proposed model for membrane disturbance, interactions modulating antibacterial and hemolytic activity are discussed.

Numerous peptide venoms and antibiotics, such as melittin (Habermann, 1972), cecropins (Hultmark et al., 1980), magainins (Zasloff, 1987), and defensins (Lehrer et al., 1993), have been isolated from the defense systems of insects, amphibians, and mammals. These peptides appear to act by enhancing the permeability of the biological membrane due to interactions with the lipid matrix. On the basis of investigations of peptide interaction with model lipid bilayers using a variety of biophysical methods, a positive net charge and a potentially amphipathic α-helix have been recognized as the major structural motifs which determine the membrane-disturbing activity of such linear peptides. Enhanced membrane permeability has been associated with enhanced binding by increasing the net positive charge of peptides, as shown for melittin (Habermann et al., 1970) and magainin (Besalle et al., 1992), and has been found to correlate with increasing amphipathic α-helical structure as demonstrated for magainin (Chen et al., 1988) and cecropin (Grazit et al., 1995). Furthermore, in recent empirical studies the total hydrophobicity of peptides of this type (Maloy et al., 1995) and the hydrophobic moment of amphipathic helices (Zhong et al., 1995) have been shown to provide a basis for modification of membrane activity. Finally, amphipathic helices exhibiting a broad nonpolar and narrow polar face have been found to encourage membrane-perturbing effects, whereas peptides comprising a broad polar and narrow nonpolar helical face are expected to enhance membrane stability (Epand et al., 1995). Concerning the size of the peptides, potential helices as short as 13 amino acid residues exhibit high membrane activity (Sitaram et al., 1995).

The mechanism discussed for the mode of action includes (i) preferential binding of the cationic peptides at charged head groups of membrane lipids and parallel orientation of the amphipathic helix in the outer bilayer leaflet with the polar face exposed to the surface and the nonpolar residues being into contact to the inner bilayer region and (ii) redistribution into the membrane and disruption of the lipid matrix or association of peptides to ion gating transmembranal pores [for review see Sansom (1991), Cornut et al. (1993), and Saberwal et al. (1994)].

Despite common structural motifs, the effect of peptide venoms and antibiotics on biological membrane systems was found to be highly differentiated. All peptides of this type kill most strains of bacteria as well as some fungi and protozoa. Some of the peptides possess antimicrobial activity and lyse erythrocytes and other eukaryotic cells [melittin (Katsu et al., 1989)], whereas others exhibit low activity against normal eukaryotic cells but are highly active against certain tumor cells [magainins and cecropins (Cruciani et al., 1991; Lincke et al., 1990; Baker et al., 1993)].

* To whom correspondence should be addressed.
‡ Institute of Molecular Pharmacology.
§ Kyoto University.
⊗ Abstract published in *Advance ACS Abstracts,* September 1, 1996.

S0006-2960(96)00835-5 CCC: $12.00

Table 1: Helical Wheel Representation of KLAL and Sequences of the Double D-Amino Acid Substitution Set and Analogs of Modified Hydrophobicity [a]

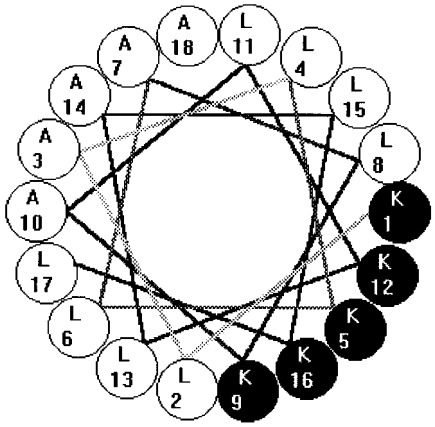

abbreviation	sequence																
KLAL	K	L	A	L	K	L	A	L	K	A	L	K	A	A	L	K	L	A
k1/l2	*k*	*l*	A	L	K	L	A	L	K	A	L	K	A	A	L	K	L	A
a3/l4	K	L	*a*	*l*	K	L	A	L	K	A	L	K	A	A	L	K	L	A
k5/l6	K	L	A	L	*k*	*l*	A	L	K	A	L	K	A	A	L	K	L	A
a7/l8	K	L	A	L	K	L	*a*	*l*	K	A	L	K	A	A	L	K	L	A
k9/a10	K	L	A	L	K	L	A	L	*k*	*a*	L	K	A	A	L	K	L	A
l11/k12	K	L	A	L	K	L	A	L	K	A	*l*	*k*	A	A	L	K	L	A
a13/a14	K	L	A	L	K	L	A	L	K	A	L	K	*a*	*a*	L	K	L	A
l15/k16	K	L	A	L	K	L	A	L	K	A	L	K	A	A	*l*	*k*	L	A
l17/a18	K	L	A	L	K	L	A	L	K	A	L	K	A	A	L	K	*l*	*a*
KLA1	K	L	A	L	K	L	A	L	K	A	W	K	A	A	L	K	L	A
KLA2	K	L	A	L	K	A	A	L	K	A	W	K	A	A	A	L	L	A
KLA3	K	L	A	L	K	A	A	A	K	A	W	K	A	A	A	K	A	A

[a] The one-letter code is used. Small letters refer to D-amino acid residues.

Recent investigations to elucidate the role of lipid composition for the activity and selectivity of peptides such as magainins and melittin led to the suggestion that differences in the amount of acidic membrane phospholipids and cholesterol play a decisive role for specificity (Matsuzaki et al., 1995; Tytler et al., 1995).

Since the secondary structures of lytic antibiotics and venoms are very similar, we consider the possibility that the varied membrane activity is due to subtle differences in the properties of the two groups of lytic peptides and determined by a sensitive balance of the structural motifs. Studies directed toward the relationship between peptide structure and activity would therefore be of considerable interest. A separate analysis of the structural features which are responsible for peptide binding and membrane insertion should help to elucidate the mechanism of action and can provide a basis for devising new systems showing enhanced and selective activity. Most of the peptide analogs synthesized so far in order to study the relationship between structure and activity are based on manipulations of the primary structure which are connected with simultaneous changes of all structural motifs such as helical propensity, net charge, or total hydrophobicity (Suenaga et al., 1989; Blondelle et al., 1991, 1992; Cornut et al., 1994). No systematic approach to understanding the role of the individual motif for peptide interaction with lipid membranes has been described. On the basis of the significance of the amphipathic helix and a positive charge, we designed a membrane-active model peptide which provides a basis for separate systematic variation of each important structural feature.

This work is aimed at uncovering the role of the amphipathic peptide helix for binding at and induction of permeability of lipid bilayers as well as the function of bilayer surface charge. We have shown that substitution of two adjacent L-amino acid residues of a potentially helical peptide by the corresponding D-isomers results in a position-dependent gradual reduction of helicity (Krause et al., 1995). Such a modification does not change other structural parameters such as total hydrophobicity and charge distribution. In this work the model peptide and its double D-amino acid replacement set (Table 1) were used to analyze the process of binding and to determine the structure of the lipid vesicle-bound peptide by circular dichroism spectroscopy. Furthermore, the role of helix and total peptide hydrophobicity for membrane permeabilization was studied by recording the peptide-induced dye release from liposomes of different surface charge by fluorescence spectroscopy. In addition, the antibacterial and hemolytic activities of the model peptides were examined. The results provide insight into the driving forces which dominate the binding process and determine the structure of the bound peptides. The data show that different mechanisms of peptide−lipid interactions are responsible for structural defects in lipid bilayers of high and reduced negative surface charge and provide a basis for understanding the observed biological effects.

MATERIALS AND METHODS

Materials. KLAL, the corresponding D-amino acid analogs (Table 1), as well as peptides with modified hydrophobicity, W^{11}KLAL (KLA1), $A^{6,15}W^{11}$KLAL (KLA2), and $A^{6,8,15,17},W^{11}$KLAL (KLA3), were synthesized automatically by solid-phase methods using standard Fmoc chemistry in the continuous flow mode (Beyermann et al., 1992). Purification was carried out by preparative HPLC on PolyEncap A300 to give final products >95% pure by RP-HPLC[1] analysis. The peptides were characterized by MALDI−MS and quantitative amino acid analysis. All lipids were purchased from Avanti Polar Lipids, Inc. (Alabaster, AL). Trifluoroethanol (TFE) was obtained from Aldrich-Chemie (Steinheim, Germany), and calcein was from Fluka Chemie (Neu-Ulm, Germany). Tris(hydroxymethyl)aminomethane (Tris) and other chemicals were from Merck (Darmstadt, Germany).

Vesicle Preparation. Small unilamellar vesicles (SUVs) for CD measurements were prepared by suspending and vortexing the dried lipid in buffer (10 mM Tris, 154 mM NaF, 0.1 mM EDTA, pH 7.4) to give final lipid concentrations between 20 and 40 mM. The suspensions were sonicated (under nitrogen in an ice bath) for 25 min using a titanium tip ultrasonicator. Titanium debris was removed by centrifugation. Dynamic light-scattering experiments (N4 Plus, Coulter Corporation, Miami, FL) confirmed the existence of a main population of vesicles (more than 95% mass content) with mean diameter of 46 ± 1 nm (polydispersity index 0.3). Large unilamellar vesicles (LUVs) for dye release experiments were prepared as follows: After vortexing the dried lipid in calcein buffer solution (70 mM calcein, 10 mM Tris, 154 mM NaCl, 0.1 mM EDTA, pH 7.4) the suspension was freeze−thawed in liquid nitrogen for seven cycles and extruded through polycarbonate filters (six times through two stacked 0.4 μm filters followed by eight times through two stacked 0.1 μm pore size filters) using a thermobarrel extruder (Lipex Biomembranes Inc., Vancouver, Canada). Untrapped calcein was removed from the vesicles by gel filtration on a Sephadex G75 column. The lipid concentration was determined by phosphorus analysis (Böttcher et al., 1961).

Circular Dichroism (CD) Measurements. Stock peptide solutions were prepared by dissolving the samples in buffer. The solution was mixed with TFE or SUV suspensions to reach the desired peptide concentration and solvent composition. CD measurements were carried out on a J 720 spectrometer (Jasco, Japan) between 185 and 260 nm at room temperature. Usually six CD scans were accumulated for each sample, and at least two independent preparations for each type of sample were measured, smoothed, and averaged. Circular dichroism and differential scattering of the SUVs were eliminated by subtracting the lipid spectra of the corresponding peptide-free suspensions. The helicity was determined from the mean residue ellipticity [Θ] at 222 nm according to the relation $[\Theta]_{222} = -30300[\alpha] - 2340$ (where [α] is the amount of helix) (Chen et al., 1972). The error was 5% helicity.

Binding Isotherms. CD spectroscopically derived binding isotherms were determined from the changes of the CD of peptide solutions (three different concentrations between 5×10^{-5} and 5×10^{-6} mol/L) after adding different amounts of SUVs. The indirect method was used for two reasons: It does not require the separation of bound and free peptide and the high sensitivity of the CD with respect to conformational changes as result of binding allows the analysis without introduction of special markers. Using for the CD of the peptide the relations: $\Phi = \Theta_{222}(0) - \Theta_{222}$ [where Φ is the relative signal, $\Theta_{222}(0)$ is the ellipticity at 222 nm in the absence of lipid, and Θ_{222} is the measured ellipticity in the presence of lipid] and $\Phi = \Phi_\infty(C_b/C_p) = \Phi_\infty(C_l/C_p)r$ [where Φ_∞ is Φ of the completely bound peptide, C_l is the lipid concentration, C_p is the total peptide concentration, C_b is the lipid-associated peptide concentration, and $r = C_b/C_l$], Φ can be plotted against C_l/C_p. From these equations and the mass conservation equation the binding isotherm can be evaluated (Schwarz & Beschiaschvili, 1989). As an approximation peptide binding at low r values can be described in terms of a partition equilibrium. In the presence of negatively charged lipids increasing binding of cationic peptides weakens electrostatic interactions, which will cause a downward curvature of the binding isotherms at higher r (Beschiaschvili & Seelig, 1990). To eliminate this effect, we evaluated the apparent binding constants which are considered to represent the affinity of the peptides to the different lipid bilayers from the initial slope of the isotherms.

Calcein Release. 10 μL of LUV suspensions was injected into a quartz cuvette containing magnetically stirred peptide solutions of different concentration to give a final volume of 2600 μL. Calcein release from the vesicles was monitored fluorimetrically by measuring the decrease in self-quenching (excitation 490 nm, emission 520 nm) at room temperature on a Perkin/Elmer LS 50B spectrofluorimeter. The fluorescence intensity corresponding to 100% leakage was determined by the addition of 100 μL of 10% Triton X-100 solution usually after 5 min of fluorescence registration. Percent leakage, F(%), after 1 min was calculated by the equation $100(\%)(I - I_0)/(I_{100\%} - I_0)$, where I is the intensity observed in the peptide solution, and I_0 and $I_{100\%}$ are the fluorescence intensities measured in the absence of peptide and in the presence of Triton X-100, respectively. Peptide concentrations causing 50% dye efflux, EC_{50}, were estimated from dose−response curves.

Dye release, F(%) as function of bound peptide per lipid, r was determined as described (Matsuzaki et al., 1989). Dose−response curves were determined by measuring dye release induced by KLAL, k9/a10, and 117/a18 from POPG and POPC LUVs at three lipid concentrations, C_l, generally 12, 24, and 36 μM. Plotting the total peptide concentration, C_p, as a function of lipid concentration for a given F(%) gives a straight line. According to the relation $C_p = rC_l + C_f$, where C_f is the concentration of free peptide, the slope of each line gives the degree of binding corresponding to the given percentage of dye release.

Antibacterial Studies. *Escherichia coli* (ATCC 8739 and DH 5α strain) were used as model Gram-negative bacteria, and *Staphylococcus epidermidis* (ATCC 12228) were used as model Gram-positive bacteria. To determine the peptide-

[1] Abbrevations: CD, circular dichroism; LUVs, large unilamellar vesicles; MALDI−MS, matrix assisted laser desorption/ionization mass spectrometry; MIC, minimal inhibition concentration; POPC, 1-palmitoyl-2-oleoyl-*sn*-glycero-3-phosphatidylcholine; POPG, 1-palmitoyl-2-oleoylphosphatidyl-DL-glycerol; RBC, red blood cells; RP-HPLC, reversed phase high-performance liquid chromatography; SDS, sodium dodecyl sulfate; SUVs, small unilamellar vesicles; TFE, 2,2,2-trifluoroethanol; Tris, tris(hydroxmethyl)aminomethane.

induced growth inhibition on the *E. coli* DH 5α strain, the cells were grown in Luria Broth (LB). A 2 mL culture was incubated overnight at 37 °C with gentle shaking (150 rpm) and diluted with 200 mL of LB to give solution showing an optical density at 540 nm (OD_{540}) of 0.05. After further incubation to reach the middle-log phase ($OD_{540} = 0.5$), the culture was divided into 10 mL fractions and the appropriate peptide dissolved in water was added immediately to each fraction in order to give a final peptide concentration of 10^{-6} mol/L. One 10 mL culture left without any treatment and one to which only water was added served as controls. After 3 h of further incubation the OD_{540} of all cell suspensions was measured using a Lambda 9 spectrometer (Perkin/Elmer Corp., Überlingen, Germany). Growth of bacteria, *G*(%) was calculated from the optical densities of the peptide-treated cultures as compared to the control. Values determined in repeat experiments differed by less than 5%.

Determination of the mean inhibition concentration of the KLAL-peptides on *E. coli* ATCC 8739 cells and *S. epidermidis* ATCC 12228 cells was carried out as recently described (Matsuzaki et al., 1994). The bacteria were grown in a medium containing the nutrients 10 g of casein peptone/L, 5 g of yeast extract/L, and 10 g of NaCl/L at 37 °C. The cells were then harvested in the mid-logarithmic phase and resuspended in a Hepes buffer (10 mM Hepes, 150 mM NaCl, 0.1 mM KCl, pH 7.0). Peptides were dissolved in the Hepes buffer and sterilized. The bacterial cells were mixed with each peptide and the medium in a microplate well. The final composition of the bacterial suspension was 10 mM Hepes, 150 mM NaCl, 1% (w/v) casein peptone, 0.5% (w/v) yeast extract, 0−320 μM peptide, and 106 cfu/mL of cells (pH 7.0). Bacterial growth was measured by the increase in optical density at 405 nm after incubation at 37 °C for 8 h (*E. coli*) and 24 h (*S. epidermidis*). The minimal inhibition concentration (MIC) was defined as the lowest concentration of peptide at which there was no change in optical density.

Hemolytic Assay. The hemolytic activity of the peptides was determined using human red blood cells (RBC) (Blutspendedienst des DRK, Berlin). The erythrocytes were washed three times in buffered saline (10 mM Tris, 150 mM NaCl, pH 7.4) just prior to the assay. The final cell concentration was 1.9×10^9 per mL. The cell suspension (200 μL) and varying amounts of peptide stock solution (concentration usually 10^{-4} mol/L in Tris buffer) and buffer were pipetted into Eppendorf tubes to give a final volume of 1500 μL. The suspensions containing 2.5×10^8 cells/mL were incubated for 30 min with gentle shaking in the Eppendorf thermomixer. After cooling in ice water and centrifugation at 2000*g* and 4 °C for 5 min, 200 μL of supernatant was dissolved with 1800 μL of 0.5% NH_4OH, and the optical density (OD_{540}) was determined in a 10 mm cuvette at 540 nm using a Lambda 9 spectrometer (Perkin/Elmer Corp., Überlingen, Germany). Zero hemolysis (blank) and 100% hemolysis (control) were determined using the supernatants after centrifugation of 200 μL of the erythrocyte stock suspension diluted and incubated in 1300 μL of buffer and 0.5% NH_4OH, respectively. Peptide concentrations causing 50% and 25% hemolysis (EC_{50} and EC_{25}, respectively) were derived from the dose−response curves. Values determined in repeat experiments differed by less than 5%.

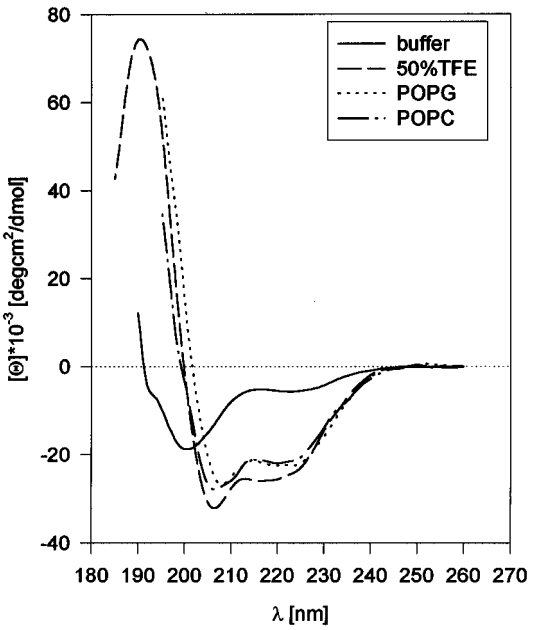

FIGURE 1: CD spectra of KLAL (peptide concentration, 10^{-5} M) in Tris buffer (—); buffer/TFE 50/50 (% v/v) (− −); buffered POPG SUV suspension (lipid concentration 2.3 mM) (···); buffered POPC SUV suspension (lipid concentration 2.0 mM) (—·—).

RESULTS

Conformation in TFE. Figure 1 shows the CD spectra of KLAL in buffer and under different structure-inducing conditions. KLAL as well as the double D-amino acid substituted analogs (spectra not shown) exhibit in buffer the spectrum of conformationally flexible peptides. Addition of TFE induces an α-helical conformation as reflected by the negative ellipticity at 207 and 222 nm and the positive CD band below 200 nm. The helical content of KLAL was determined to be 72%. Figure 2 shows that introduction of two adjacent D-amino acid residues drastically reduces the helical order. Substitutions in the center of the chain are most effective. Recently published CD investigations of the double D-amino acid substituion set in acidic TFE/water mixtures (Krause et al., 1995) suggested that the helix comprises the entire KLAL chain with reduced stability at the N- and C-termini caused by the helix end effect (Chakrabartty et al., 1991).

Helicity in Suspensions of POPG, Mixed POPG/POPC, and POPC Vesicles. Interaction of KLAL with SUVs composed of negatively charged POPG is connected with helix formation (Figure 1). The helical content of the vesicle-bound peptide was calculated to be 62% ± 2%. With the exception of double D-amino acid substitutions in the N-terminus all modifications resulted in helix disturbance which was slightly more pronounced in the C-terminal half of the peptide chain (Figure 3a). Titration experiments of KLAL and k9/a10 solutions with POPG SUVs confirmed that the CD spectra used as a basis for the structural calculations actually reflect the conformation of the bound peptides. At lipid concentrations between 10^{-4} and 2.3×10^{-3} M the CD spectra of KLAL as well as that of the less helical analog, k9/a10 (peptide concentration, 10^{-5} M) were superimposed, showing that even at the very low POPG/peptide ratio (C_l/C_p) of 10 the two cationic peptides are completely bound.

With reduction of the negative vesicle surface charge (POPG/POPC = 1/3 mol/mol) the binding affinities of the

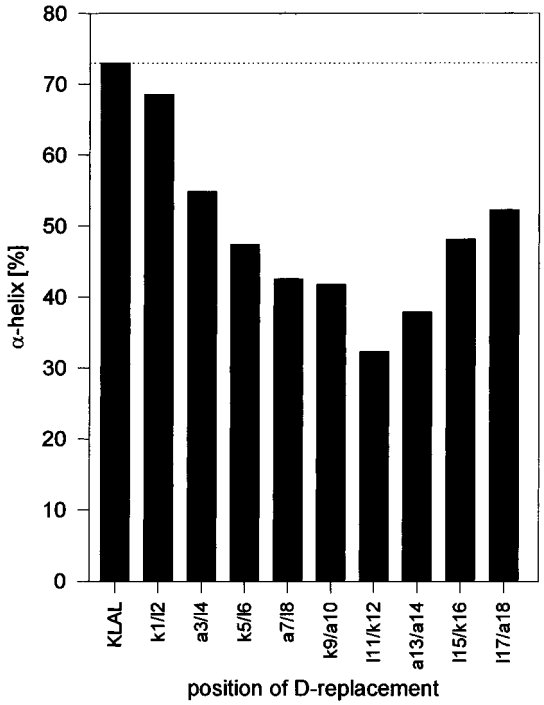

FIGURE 2: Helicity, α(%), of KLAL and the double D-amino acid substituted analogs in Tris buffer/TFE = 50/50 (% v/v) at peptide concentration of 10^{-5} M.

peptides decrease and binding of KLAL and k9/a10 becomes more differentiated (Figure 4). The apparent binding constants derived from the initial slope of the binding isotherms (Figure 4) are 2.6×10^4 and 1.5×10^4 M^{-1}, respectively. KLAL also exhibits high helicity in the presence of mixed POPG/POPC vesicles and SUVs composed of zwitterionic POPC (Figure 3b, Table 2). Figure 3b shows the helical profile of the complete substitution set in the presence of pure POPC liposomes. Binding studies reveal that accumulation of KLAL at POPC-vesicles is very low (Figure 4). The apparent binding constant, K_{app} of KLAL was determined to be about 10^3 M^{-1}. Upon titration of a 10^{-5} M KLAL solution with POPC SUVs, constant ellipticity values were reached only at lipid concentrations higher than 5 mM showing that only beyond a lipid/peptide ratio of 500 are the peptide molecules almost completely bound. As a consequence, under the experimental conditions used for structural investigations of the substitution set ($C_l/C_p = 200$) (Figure 3b) not all KLAL molecules were in the lipid-bound state. The low affinity of KLAL peptides at POPC vesicles further decreases with double D-amino acid substitution, as shown for k9/a10. By increasing the POPC/k9/a10 ratio up to 1100 the CD spectrum of the analog studied (peptide concentration 10^{-5} mol/L) continuously changed, thus reflecting a continuously increasing amount of bound peptide (spectra not shown). Consequently, the helical profile of Figure 3b reflects different peptide binding as a result of helix disturbance rather than differences in the structure of the POPC-bound KLAL peptides.

The surface charge density of the vesicle was found to influence only slightly the CD characteristics and structure of bound KLAL peptides (Table 2). Differences in the helical content of KLAL bound at POPG, mixed POPG/POPC and POPC vesicles are small. Also the helicity of bound k9/a10 does not change with reduction of the negative charge density as shown for POPG and POPC/POPG liposomes (Table 2). The nonhelical structure of k9/a10 in the presence of POPC vesicles shows that the peptide is not bound.

Membrane-Disturbing Activity. An important feature of the dye release curves is the fact that fluorescence intensity reaches a plateau a few minutes after addition of POPG vesicles to the peptide solution (data not shown). Figure 5a compares the effect of the KLAL peptides on the membrane permeability of POPG LUVs. The peptide concentration inducing 50% calcein release after 1 min, EC_{50}, at a lipid concentration of 12 μM was found to range between 0.1 and about 1 μM. Differences in the induction of vesicle permeability are small, and there is no correlation with helical propensity determined in structure inducing TFE environment (Figure 2) or helicity of the POPG-bound peptides (Figure 3a). Comparing KLAL, k9/a10, and l17/a18, the bilayer-

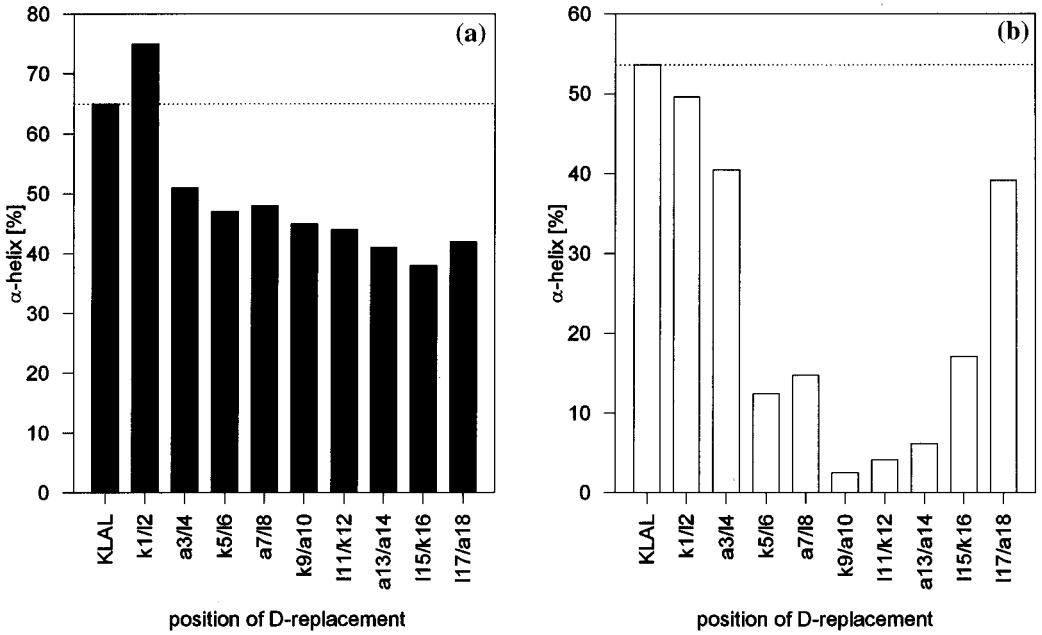

FIGURE 3: Helicity, α(%), of KLAL and the double D-amino acid substituted analogs in presence of POPG SUVs (a) (lipid concentration, 2.3 mM) and POPC SUVs (b) (lipid concentration, 2.0 mM) at peptide concentration of 10^{-5} M in Tris buffer.

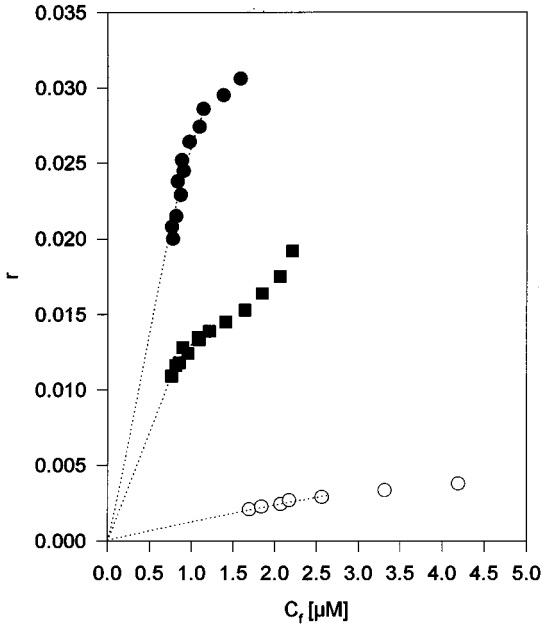

FIGURE 4: Binding isotherms of KLAL (●) and k9/a10 (■) at mixed POPG/POPC (1/3 mol/mol) SUVs and of KLAL (○) at POPC SUVs in Tris buffer at 23 °C (*r* is the amount of peptide bound per lipid and C_f is the concentration of free peptide). The isotherms were derived from CD spectroscopic experiments as described by Schwarz et al. (1989). The dotted lines correspond to a partition equilibrium.

disturbing activity follows the order k9/a10 > KLAL > l17/a18, whereas helical propability decreases in the order KLAL > l17/a18 > k9/a10 and that of POPG-bound helical content in the order KLAL > k9/a10 > l17/a18.

In contrast, the activity profile of the substitution set on POPC liposomes is highly pronounced (Figure 5b). While the concentration for half-maximal dye release of KLAL was 2.5×10^{-8} M, the concentration of the least effective peptide (k9/a10) was found to be about 50 times higher (1.3×10^{-6} M). The permeabilizing activity correlated well with the helical content of KLAL peptides in the TFE/buffer system

Table 2: Mean Residue Ellipticity, [Θ] at 222 nm, and Calculated Helicity, α(%), of KLAL and k9/a10 in POPG, Mixed POPG/POPC, and POPC SUV Suspensions at Lipid Concentrations C_l[a]

	$[\Theta]_{222}/\alpha(\%)$		
peptide	POPG ($C_l = 2.3 \times 10^{-3}$ M)	POPG/POPC (1/3 mol/mol) ($C_l = 2.2 \times 10^{-3}$ M)	POPC ($C_l = 10 \times 10^{-3}$ M)
KLAL	−21 000/62	−21 000/63	−22 600/67
k9/a10	−16 555/46	−15 500/43	−3 100/3[b]

[a] The peptide concentration was 10^{-5} M in 10 mM Tris buffer, 154 mM NaF, 0.1 mM EDTA, pH 7.4. [b] All values except this one represent conformational properties of vesicle-bound peptides.

(Figure 2) as well as with the affinity and helicity in the presence of POPC liposomes (Figure 3b). Most surprising was the observation that the membrane-disturbing effect of the various peptides having high inherent helicity (KLAL or l17/a18) significantly increases with reduction of the negative surface charge of the liposomes (Figure 6). This is especially impressive, since KLAL peptides have been found to exhibit a decreasing binding affinity upon reduction of the negative surface charge of the vesicles. Table 3 summarizes the *r*-values (amount of peptide bound per lipid molecule) for representative KLAL peptides causing half-maximal calcein release. While the induction of 50% release from POPG vesicles by KLAL and l17/a19 is reached at a binding of 29 and 94 peptide molecules per 1000 lipid molecules, respectively, binding of three to four peptide molecules per 1000 lipid molecules is sufficient to induce the same dye efflux from POPC liposomes. It is clear that binding of these KLAL peptides as a function of vesicle charge does not correlate with the permeabilizing activity. In contrast, vesicle permeability effects of the less helical peptide k9/a10 decrease with reduction of the negative charge density of the liposomes (Figure 6, Table 3). The EC_{50} of dye release increases from 0.1 μM at POPG liposomes to 1.3 μM at POPC vesicles, corresponding to amounts of membrane-associated peptide per lipid of 0.01 and 0.117, respectively. The effect correlates with the low membrane

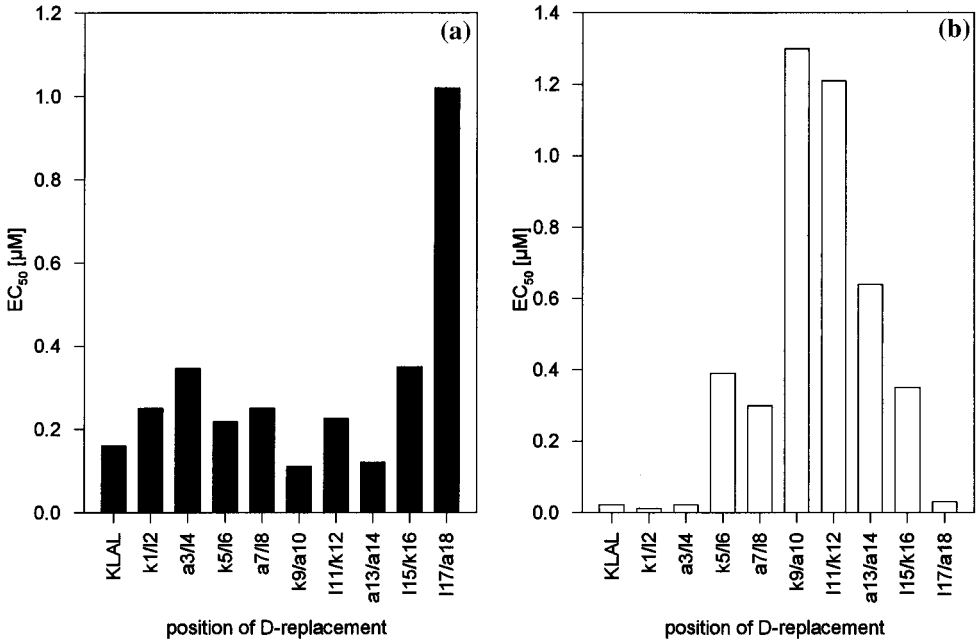

FIGURE 5: Lipid membrane-disturbing effect of the KLAL substitution set. Concentration of half-maximal dye release (EC_{50}) out of POPG LUVs (a) and POPC LUVs (b) induced by KLAL peptides at lipid concentration of 12 μM. EC_{50} data were derived from fluorescence spectroscopically detected calcein release at different peptide concentrations after 1 min (see also Figure 7).

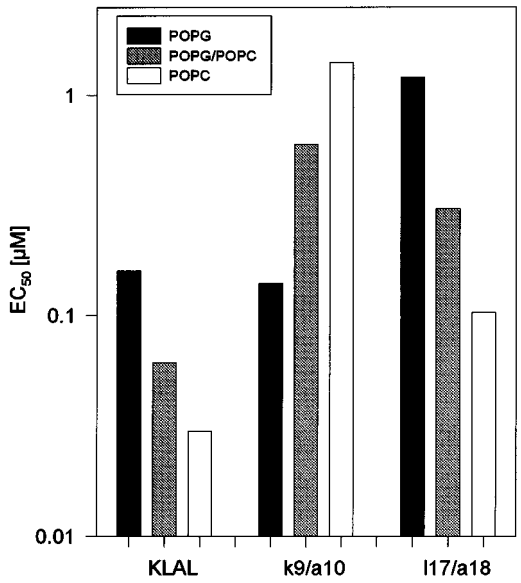

FIGURE 6: EC_{50} of dye release induced by KLAL, k9/a10, and l17/a18 from POPG LUVs (black bars), mixed POPG/POPC (1/3 mol/mol) LUVs (shadowed bars), and POPC LUVs (open bars). The lipid concentration was 12 μM in 10 mM Tris buffer, 154 mM NaCl, 0.1 mM EDTA, pH 7.4.

Table 3: Amount of Peptide (KLAL, k9/a10, l17/a18) Bound per Lipid, *r* Causing Half-Maximal Dye Release [*F*(50%)] from POPC and POPG LUVs [a]

	$r_{F(50\%)}$	
peptide	POPC	POPG
KLAL	0.003	0.029
k9/a10	0.117	0.010
l17/a18	0.004	0.094

affinity of the less helical analogs at vesicles of low negative surface charge.

Results of investigations performed to confirm the decisive role of the hydrophobic helix domain for peptide interactions with bilayers composed of zwitterionic lipids are given in Table 4. The three KLAL analogs, KLA1, KLA2, and KLA3, of different hydrophobicity are identical with respect to their helix-forming capacity (helicity in 50% TFE) and do not show drastic differences in helicity in the presence of POPG vesicles or in POPG bilayer-disturbing activity. However, the helical content of the three peptides determined in POPC vesicle suspensions and the EC_{25} of peptide-induced dye release out of POPC liposomes are distinctly different. Both helicity and membrane-disturbing activity strongly correlate with peptide hydrophobicity.

Biological Effects. Figure 7 and Table 5 show that KLAL exhibits high antibacterial as well as high hemolytic activity. Double D-amino acid substitution modulates these effects. The minimal inhibition concentration on Gram-negative and Gram-positive bacteria is in the micromolar range. In comparison to the KLAL-treated *E. coli* (peptide concentration, 1 μM), which exhibit a reduced growth ($G = 60\%$) compared to the nontreated control ($G = 100\%$), amino acid substitution reduces the growth-inhibiting effect of the peptide (Figure 7a). The minimal inhibition concentrations of KLAL (4×10^{-6} M) and the least effective analogs (32×10^{-6} M) differ by a factor of 8 (Table 5). The effect of KLAL peptides on *S. epidermidis* was found in the same range, although the activity profile of the substitution set is slightly different. Least effective in growth inhibition are sequences modified in the center of the peptide chain such as k9/a10 and l11/k12 (Table 5) which also show low helicity. A concentration of 5×10^{-5} M KLAL causes complete lysis of human erythrocytes (cell concentration, 2.5×10^8 per mL) (Figure 7b). Double D-amino acid substitution drastically reduces the effect. With the exception of substitution in positions 1/2 and 3/4, the analogs exhibit a pronounced loss of hemolytic activity. The effect of substitution becomes more impressive upon comparing the EC_{50} (Table 5). We observed a pronounced activity profile which exhibited maximum differences in the EC_{50} of a factor of 80, showing that the analogs of lowest helical content (Figure 2) were the least effective.

DISCUSSION

Our approach to studying the role of the amphipathic helix for peptide binding and membrane disturbance and searching for the relation between peptide helicity and antibacterial and hemolytic activity has been based on a cationic 18-mer model peptide which is capable of forming an idealized amphipathic helix with the five lysine side chains covering an angle of about 90° of the helical coat. The mean hydrophobicity and the hydrophobic moment per residue, calculated to be −0.016 and 0.334, respectively (Eisenberg, 1984) are representative for membrane-active compounds.

The basis for the interpretation of the interaction studies of the KLAL peptides with simple membrane model systems and biological cells is the observation that substitution of two adjacent amino acid residues by their D-isomers results in CD spectroscopically detectable changes of the helicity. The helical profile of KLAL, previously described in acidic TFE/water mixtures (Krause et al., 1995) and now confirmed in a neutral TFE/buffer system (Figure 2) shows a pronounced reduction of helicity with substitution in the center of the chain. Assuming that the degree of disturbance of the helix can be correlated with helix stability in the replaced peptide region, the pronounced profile observed led to the

Table 4: Properties of KLAL Peptides of Different Hydrophobicities [a]

				POPG		POPC	
peptide	*H*	μ	α(%) 50% TFE[b]	α(%) $C_l/C_p = 500$[b]	EC_{50} (M) $C_l = 1.2 \times 10^{-5}$ M[c]	α(%) $C_l/C_p = 500$[b]	EC_{25} (M) $C_l = 1.2 \times 10^{-5}$ M[c]
KLAL	−0.016	0.334	72	62	0.23×10^{-6}	65	2.5×10^{-8}
KLA1	−0.025	0.329	73	54	0.25×10^{-6}	59	9×10^{-9}
KLA2	−0.056	0.329	68	45	0.29×10^{-6}	23	6×10^{-7}
KLA3	−0.087	0.329	69	43	0.35×10^{-6}	0	9.2×10^{-5}

[a] *H*, hydrophobicity; μ, hydrophobic moment calculated as described by Eisenberg (1984). Helicity, α(%), in Tris buffer/TFE = 50/50 (% v/v) and in POPC and POPG SUV suspension (10 mM Tris buffer, 154 mM NaF, pH 7.4) at a lipid/peptide ratio, C_l/C_p, of 500. [b] The peptide concentration was 10^{-5} M. [c] EC_{25} and EC_{50}, peptide concentration causing 25% and 50% dye release, respectively, after 1 min from POPC and POPG LUVs at lipid concentration, C_l of 12 μM suspended in 10 mM Tris buffer, 154 mM NaCl, 0.1 mM EDTA, pH 7.4.

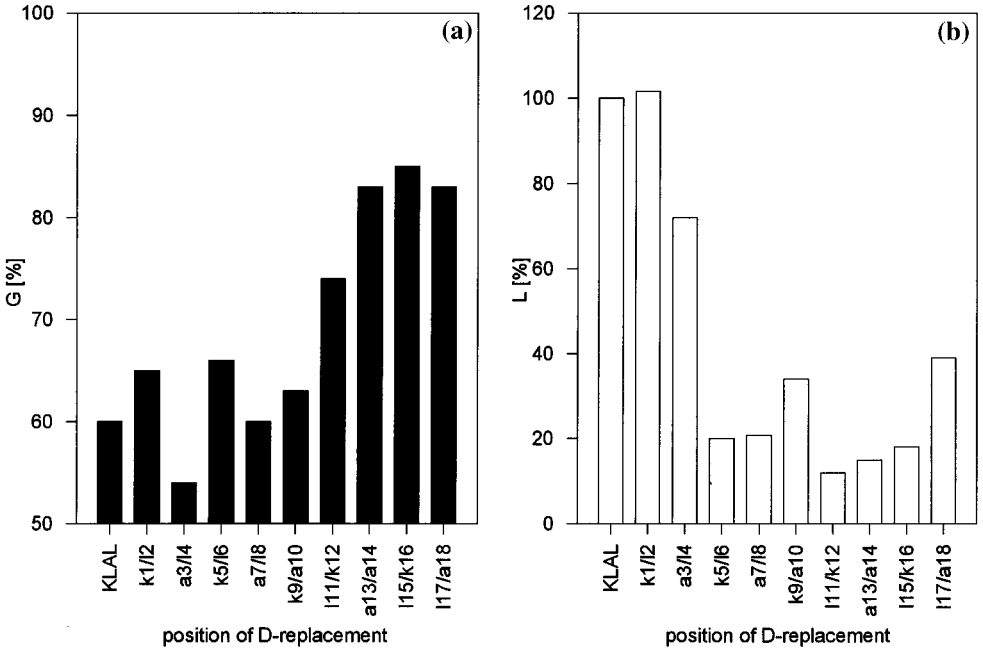

FIGURE 7: (a) Antibacterial activity of the KLAL replacement set (black bars). Influence of KLAL peptides on the growth, *G*(%), of *E. coli* (DH 5α) at a peptide concentration of 1 μM after 3 h of incubation at 37 °C in Luria Broth. The growth of the untreated control was set at 100%. Values obtained in repeat determinations differed by less than 5%. (b) Hemolytic activity of the KLAL replacement set (white bars). Percent lysis of erythrocytes, *L*(%), induced by KLAL peptides at a peptide concentration of 50 μM. The cells (2.5×10^8 per mL) were suspended in 10 mM Tris buffer, 150 mM NaCl, pH 7.4, and incubated for 30 min at 37 °C. Values determined in repeat experiments differed by less than 5%.

Table 5: Minimal inhibition concentration (MIC) of KLAL peptides on *E. coli* and *S. epidermidis bacteria* and EC_{50} of the hemolytic effect of KLAL peptides on human red blood cells (RBC)

	MIC (μM)[a]		EC_{50} (μM)[b]
peptide	*E. coli*	*S. epidermidis*	human RBC
KLAL	4	2	10
k1/l2	4	4	7
a3/l4	8	2	33
k5/l6	8	4	160
a7/l8	8	2	180
k9/a10	16	16	56
l11/k12	32	32	540
a13/a14	16	8	260
l15/k16	32	8	210
l17/a18	16	4	70

[a] Determined by measuring the optical density at 405 nm after 8 h (*E. coli*) and 24 h (*S. epidermidis*) of incubation at 37 °C at peptide concentrations of 2, 4, 8, 16, 32, and 64 μM. [b] Determined by measuring the optical density at 540 nm after 30 min of incubation of 2.5×10^8 cells/mL at 37 °C in 10 mM Tris buffer, 150 mM NaCl, pH 7.4. All values determined in repeat experiments differed by less than 5%.

suggestion that the helix comprises the entire peptide chain and exhibits a high stability which is weakened at the N- and C-termini caused by the helix end effect (Chakrabartty et al., 1991). Following Lehrman et al. (1990), who suggested that the TFE enhanced helicity of peptides is indicative of their capability to form a helix, we take the helical profile in Figure 2 as an expression of the helical propensity of KLAL peptides.

Our investigations of peptide interaction with lipid bilayers show that the potentially amphipathic model compound, KLAL binds at membrane interfaces for two reasons: (i) electrostatic interactions between the cationic peptide charges and the anionic lipid head groups of the membrane and (ii) hydrophobic interactions between the hydrophobic domains of the peptide and the hydrocarbon chains of the lipid. This folding from the initial random coil in solution to a highly ordered conformation strongly depends on the nature of the lipid bilayer environment (Zhong et al., 1992).

CD spectra of KLAL as well as those of a representative analog of reduced helicity, k9/a10, did not show any differences in helix character upon reducing the POPG/peptide ratio from 200 to 10 showing that both peptides, independent of their helical propensity, are completely bound to the negatively charged vesicles. The peptide accumulation at the bilayer is independent of their capability to form a helix revealing that the amphipathic helix domain plays a negligible role in the interaction process. Electrostatic interactions between the peptide charges and lipid head groups predominate in the binding process. The helicity of POPG-bound KLAL is about 63%. However, in contrast to the pronounced helical profile of the KLAL substitution set in a TFE/buffer mixture (Figure 2) the various analogs exhibit only slightly reduced and barely differentiated helicity in the POPG-bound state (Figure 3a). We suggest that strong electrostatic interactions between the five regularly distributed charged side chains and the negatively charged lipid head groups anchor the KLAL peptides in the lipid head group/acyl chain interface of the POPG layer. It is plausible to assume that this fixation of the KLAL peptide supports the stability of the induced structure and causes reduction of the flexibility at the chain ends. Consequently, double D-amino acid substitution of two adjacent side chains should exhibit comparable helix disturbing effects independent of the position of modification thus explaining the slight differences in helicity of the bound analogs. At present we cannot offer an explanation for the comparably high helicity of k1/l2 (see Figure 3a), although we often observed an increase in helicity in peptide analogs with double D-amino acid substitution in the beginning of a potentially amphipathic

helix region when interacting with negatively charged vesicles or SDS micelles.

The increasing role of the amphipathic helix with reduction of bilayer surface charge shows how the balance between ionic and hydrophobic peptide−lipid interactions can be changed. Reduction of the negative surface charge of the lipid bilayer drastically reduces peptide affinity as shown by evaluation of binding isotherms of KLAL at mixed POPG/POPC vesicles and liposomes composed of zwitterionic POPC. With decrease in vesicle charge hydrophobic interactions become dominant. In addition, binding of peptides at lipid bilayers of reduced negative surface charge was found to be strongly modulated by the tendency toward helix formation. We suggest that double D-amino acid substitution modifies the size of the hydrophobic helix domain thus influencing hydrophobic peptide−lipid interactions.

The vesicle surface charge was found to be of little influence on the structure of membrane-bound KLAL leading to the conclusion that the induction of secondary structure is mainly driven by hydrophobic interactions. Taking into consideration the little-differentiated helical profile of POPG-bound KLAL peptides which reflects the structure of the completely bound sequences, the pronounced helical profile of the KLAL substitution set in interaction with POPC liposomes (Figure 3b) should reflect the dramatic changes in binding affinity of analogs of reduced helical propensity rather than differences in peptide conformation. Indeed, the profile correlates well with the retention time profile of the KLAL replacement set in reversed phase HPLC (Krause et al., 1995) which is determined by varied affinities toward the hydrophobic stationary phase.

The permeability-enhancing activity of KLAL peptides toward vesicles of high negative charge density (POPG) was found to be in the submicromolar concentration range and nearly independent of the helicity in the lipid-bound state. Binding experiments showed that all peptides are completely bound at concentrations causing dye release. Our interpretation is that electrostatic interactions between the positive peptide charges and the acidic phospholipid head groups anchor the sequences at the bilayer surface. Recently, Reynaud et al. (1993) suggested the formation of lipid domains oriented around a bound peptide. We suppose that in addition strong ionic interactions might cause reorientation of lipid head groups and favor the formation of densely packed peptide−lipid clusters (Figure 8a). In this connection it is interesting to note that melittin, which exhibits a behavior at lipid bilayers which is comparable to that of our model compound, was found to be one of the most effective lipid head group modulators (Beschiaschvili et al., 1990). The slight differences observed in the activity of the analogs (Figure 5a, Table 3) could be associated with different spatial arrangements of the charged residues in the lipid head group region, thus resulting in different peptide surface areas and differently organized peptide−lipid clusters.

Most surprising was the observation that despite low affinity the effect of helical KLAL on permeability substantially increased at bilayers of reduced surface charge. Such an increase of activity is clearly not caused by enhanced peptide accumulation. We suppose that with reduction of electrostatic peptide−lipid interactions, hydrophobic interactions favor the transfer of the peptides from the bilayer surface into the nonpolar acyl chain region as illustrated in Figure 8b. Comparable observations have recently been published for melittin (Benachir et al., 1995; Monette et al., 1995) and mastoparan peptides (Park et al., 1995). Recently, Reynaud et al. (1994) proposed a model for pore formation by cationic amphipathic model peptides in phosphatidylcholine small unilamellar vesicles, and ion channel activities of a basic amphipathic model peptide in black membrane experiments have been reported (Agawa et al., 1991). According to the theoretical work of Schwarz (1989) association of peptide monomers as prerequisite for the formation of channels is expected to be reflected by a strong upper bending of the binding isotherms. The binding curves of KLAL may be fitted through the origin and do not argue for the involvement of peptide association.

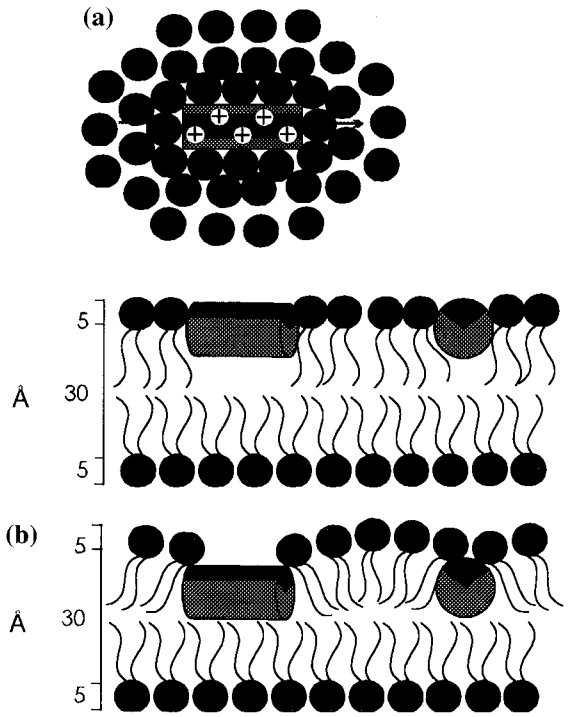

FIGURE 8: Model of interaction of the amphipathic KLAL-helix with lipid bilayers of different negative surface charge. (a) Strong electrostatic interactions between the cationic residues in the polar face of the helix and the negatively charged lipid head groups anchor the peptide in the membrane surface region, preferentially causing changes in the organization of the lipid head groups. (b) At low negative surface charge hydrophobic interactions between the hydrophobic face of the helix and the lipid acyl chains drive insertion of the peptide into the inner nonpolar membrane region, causing disturbance in the arrangement of the acyl chains.

Our results are consistent with a deeper insertion of the peptides into the bilayer which is expected to force the acyl chains apart and to disturb the membrane-stabilizing hydrophobic lipid interactions, thus causing localized disruptions. Although the manner in which this redistribution proceeds is not yet completely clear, the process is dominated by hydrophobic interactions and should depend on the size of the hydrophobic helix domain and the total hydrophobicity of the peptide. Indeed, our studies revealed that the effect of KLAL peptides on neutral bilayers parallels their intrinsic helicity. Highly helical analogs with a large hydrophobic face are much more effective than less helical sequences. In addition, studies of KLAL analogs of reduced hydrophobicity in interaction with POPC vesicles showed that reduction of membrane activity correlates with a decrease in peptide hydrophobicity thus confirming the dominating role of hydrophobic interactions. All together, disturbance of the

hydrophobic inner membrane region was found to have a more dramatic effect on membrane permeability than high peptide accumulation at the membrane surface.

The mechanism of antibiotic activity of peptides is still controversial. The absence of detailed structural information of the peptides and the complexity of the structure of the bacterial membrane seriously hamper the interpretation of biological effects. Gram-negative bacterial envelops are complex structures composed of an inner and an outer membrane with a high degree of negatively charged lipopolysaccharides located on the exterior surface of the outer membrane. The surface area of lipopolysaccharides and phospholipids in membrane systems can be approximated to be 200 Å^2 (Yeagle, 1992) and 74 Å^2 (Gennis, 1989), respectively. Assuming that the outer leaflet of the outer *E. coli* membrane is almost completely composed of lipopolysacharides bearing six negative charges (Rana et al., 1991), the negative surface charge density of the outer *E. coli* membrane was calculated to reach −30 per 1000 Å^2. The value is still much higher than that of −13.5/1000 Å^2 calculated for a pure POPG layer.

The correlation between the binding profile of the KLAL replacement set toward POPG bilayers and the activity profile toward *E. coli* suggests that the KLAL peptides exhibit high affinity for the anionic surface components of bacteria. We suppose that the bactericidal effect is initiated by disruption of the outer membrane as a result of high peptide accumulation caused by strong electrostatic peptide−lipid interactions, thus allowing the peptides to reach and disturb the inner leaflet (Christensen et al., 1988; Sansom, 1991). Gram-positive bacterial surfaces contain negative charges owing to the presence of teichoic and teichuroic acids along with the carboxyl groups of amino acids found in the peptidoglycan layer (Hammond et al., 1984). Also in this case cationic peptides are expected to bind the membranes. In fact, our KLAL peptides exhibit minimal inhibition concentrations on *S. epiderminis*, which are comparable to those observed for *E. coli*. However slight changes in the activity profile were observed (see Table 5). Unfortunately, we cannot offer an unequivocal interpretation of the slight differentiation in the activity profiles against the two classes of bacteria, other than by reference to differences in their membrane architecture. It could be that the difference reflects a reduction in negative surface charge of *S. epidermidis* compared to *E. coli*. The reduction would decrease the dominating role of electrostatic interactions and should cause changes in the activity profile of the KLAL peptides. Such an assumption is supported by lysis experiments with erythrocytes. The outer half of the erythrocyte membrane is composed mainly of neutral phosphatidylcholine and phosphatidylethanolamine and no acidic phospholipids. However, it is said that many sialic molecules are located in the outer leaflet about 80 Å from the surface (Vitala et al., 1985). It has been suggested that the anionic charges of these residues may act to keep cationic amphipathic peptides far from the red blood cell membrane (Park et al., 1995; Saberwal et al., 1994), thus preventing interaction with the lipid components and reducing membrane disturbance. However, according to our results charge interactions are less important than hydrophobic effects. The correlation between hemolytic activity and the disturbing effect of KLAL peptides of different helicity on POPC bilayers supports a direct interaction of the amphipathic peptides with the electrically neutral lipid matrix of the blood cells. Hemolytic activity is then controlled by hydrophobic interactions which allow the peptide to reach the inner hydrophobic membrane region.

In summary, we have shown different peptide−lipid interactions to be responsible for induction of permeability of model membranes bearing high and low negative surface charges. The effect on highly negatively charged lipid bilayers is determined by peptide accumulation at the membrane surface. Peptide secondary structure is of less importance. Disturbance of the lipid arrangement is expected to be caused mainly by dominating electrostatic interactions between the peptide charges and lipid headgroups. At bilayers of reduced negative surface charge membrane disturbance is dependent on the size of the hydrophobic helix domains and the total hydrophobicity revealing that it is the inner hydrophobic membrane region which is affected. On the basis of these results a model for peptide membrane interaction is suggested which also serves to provide some explanation of the selective biological effects. According to our results, peptide modifications which enhance charge interactions should cause an increase in antibacterial activity whereas reduction of electrostatic interactions and modifications compatible with increased hydrophobic peptide−lipid interactions should enhance hemolytic effects. Further studies concerning hydrophobic effects are in progess in order to confirm our interpretations.

ACKNOWLEDGMENT

The authors thank A. Klose, D. Smettan, and B. Pisarz, Institute of Molecular Pharmacology, for assistance in peptide synthesis and characterization and H. Nikolenko and L. Handel, Institute of Molecular Pharmacology, for excellent technical work in all the biophysical experiments and the hemolytic assay. L. A. Carpino, University of Massachusetts, Amherst, is thanked for a critical reading of the manuscript.

REFERENCES

Agawa, Y., Lee, S., Ono, S., Aoyagi, H., Ohno, M., Taniguchi, T., Azai, K., & Kinino, Y. (1991) *J. Biol. Chem. 260*, 20218−20222.

Baker M. A., Maloy, W. L., Zasloff, M., & Jacob, L. S. (1993) *Cancer Res. 53*, 3052−3057.

Benachir, T., & Lafleur, M. (1995) *Biochim. Biophys. Acta 1235*, 452−460.

Besalle, R., Haas, H., Goria, A., Shalit, I., & Fridhin, M. (1992) *Antimicrob. Agents Chemother. 36*, 313−317.

Beschiaschvili, G., & Seelig, J. (1990) *Biochemistry 29*, 52−58.

Beyermann, M., Wenschuh, H., Henklein, P., Bienert, M. (1992) in *Innovation and Perspectives in Solid Phase Synthesis* (Epton, R., Ed.) pp 349−353, Intercept Limited, Andover, U.K.

Blondelle, S. E., & Houghten, R. A. (1991) *Biochemistry 30*, 4671−4678.

Blondelle, S. E., & Houghten, R. A. (1992) *Biochemistry 31*, 12688−12694.

Böttcher, C. J. F., van Gent, C. M., & Pries, C. (1961) *Anal. Chim. Acta 24*, 203−204.

Chakrabartty, A., Schellmann, J. A., & Baldwin, R. L. (1991) *Nature 351*, 586−588.

Chen, H.-C., Brown, G. H., Morell, J. L., & Huang, C. M. (1988) *FEBS Lett. 236*, 462−466.

Chen, Y. J., Yang, J. T., & Martinez, H. M. (1972) *Biochemistry 11*, 4120−4131.

Christensen, B., Fink, J., Merrifield, R. B., & Mauzerall, D. (1988) *Proc. Natl. Acad. Sci. U.S.A. 85*, 5072−5076.

Cornut, I., Büttner, K., Dasseux, J.-L., & Dufourcq, J. (1994) *FEBS Lett. 349*, 29−33.

Cornut, I., Thiaudiere, E., & Dufourcq, J. (1993) in *The Amphipathic Helix* (Epand, R. M., Ed.) pp 172−220, CRC Press, Boca Raton, FL.
Cruciani, R. A., Barker, J. L., Zasloff, M., Chen, H.-C., & Colamonici, O. (1991) *Proc. Natl. Acad. Sci. U.S.A. 88*, 3792−3796.
Eisenberg, D. (1984) *Annu. Rev. Biochem. 53*, 595−623.
Epand, R. M., Shai, Y., Segrest, J. P., & Anantharamaiah, G. M. (1995) *Biopolymers 37*, 317−338.
Gennis, R. B. (1989) in *Biomembranes: Molecular Structure and Function* (Cantor, C. R., Ed.) p 82, Springer Verlag, New York.
Grazit, E., Boman, A., Boman, H. G., & Shai, Y. (1995) *Biochemistry 34*, 11479−11488.
Habermann, E. (1972) *Science 177*, 314−321.
Habermann, E., & Kowallek, H. (1970) *Hoppe-Seyler's Z. Physiol. Chem. 351*, 884−890.
Hammond, S. M., Lambert, P. A., & Rycroft, A. N. (1984) in *The Bacterial Cell Surface*, Croom Helm, London.
Hultmark, D., Steiner, H., Rasmuson, T., & Boman, H. G. (1980) *Eur. J. Biochem. 106*, 7−16.
Katsu, T., Kuroko, M., Morinawa, T., Sanchika, K., Fujita, Y., Yamamura, H., & Uda, M. (1989) *Biochim. Biophys. Acta 983*, 135−141.
Krause, E., Beyermann, M., Dathe, M., Rothemund, S., & Bienert, M. (1995) *Anal. Chem. 67*, 252−256.
Lehrer, R. I., Lichtenstein, A. K., & Ganz, T. (1993) *Annu. Rev. Immunol. 11*, 105−128.
Lehrman, S. R., Tuls, J. L., & Lund, M. (1990) *Biochemistry 29*, 5590−5596.
Lincke, C. R., Van der Bliek, A. M., Schuurkuis, G. J., Van der Velde-Koerts, T., Smit, J. J. M., & Borst, P. (1990) *Cancer Res. 50*, 1779−1785.
Maloy, W. L., & Kari, U. P. (1995) *Biopolymers 37*, 105−122.
Matsuzaki, K., Harada, M., Handa, T., Funakoshi, S., Fujii, N., Yajima, H., & Miyajima, K. (1989) *Biochim. Biophys. Acta 981*, 130−134.
Matsuzaki, K., Murase, O., Toduda, H., Funakoshi, S., Fujii, N., & Miyajima, K. (1994) *Biochemistry 33*, 3342−3349.
Matsuzaki, K., Sugishita, K.-I., Fujii, N., & Miyajima, K. (1995) *Biochemistry 34*, 3423−3429.
Monette, M., & Lafleur, M. (1995) *Biophys. J. 68*, 187−195.
Park, N. G., Yamato, Y., Lee, S., & Sugihara, G. (1994) *Biopolymer 36*, 793−801.
Rana, F. R., Macias, E. A., Sultany, C. M., Madzrakowski, C., & Blazyk, J. (1991) *Biochemistry 30*, 5858−5866.
Reynaud, J. A., & Sy, D. (1994) *Bioelectrochem. Bioenerg. 34*, 1−4.
Reynaud, J. A., Grivet, J. P., Sy, D., & Trudelle, Y. (1993) *Biochemistry 32*, 4997−5008.
Saberwal, G., & Nagaraj, R. (1994) *Biochim. Biophys. Acta 1197*, 109−131.
Sansom, M. S. P. (1991) in *Progress in Biophysics and Molecular Biology* (Noble, D., & Blundell, T. K., Eds.) Vol. 3, pp 139−235, Pergamon Press, Oxford.
Schwarz, G. (1989) *Biochemie 71*, 1−9.
Schwarz, G., & Beschiaschvili, G. (1989) *Biochim. Biophys. Acta 979*, 82−90.
Sitaram, N., Subbalakshmi, C., & Nagaraj, R. (1995) *Int. J. Pept. Protein Res. 46*, 166−173.
Suenaga, M., Lee, S., Park, N. G., Aoyagi, H., Kato, T., Umeda, A., & Amako, K. (1989) *Biochim. Biophys. Acta 981*, 143−150.
Tytler, E. M., Anantharamaiah, G. M., Walker, D. E., Mishra, V. K., Palgunachari, M. N., & Segrest, J. P. (1995) *Biochemistry 34*, 4393−4401.
Vitala, J., & Jarnefelt, J. (1985) *Trends Biochem. Sci. 12*, 392−395.
Yeagle, Ph. (1991) in *The Structure of Biological Membranes*, p 29, CRC Press, Boca Raton, FL.
Zasloff, M. (1987) *Proc. Natl. Acad. Sci. U.S.A. 84*, 5449−5453.
Zhong, L., & Johnson, W. C. (1992) *Proc. Natl. Acad. Sci. U.S.A. 89*, 4462−4465.
Zhong, L., Putnam, R. J., Johnson, W. C., & Rao, A. G. (1995) *Int. J. Pept. Protein Res. 45*, 337−347.

BI960835F